Energy and Exergy Analysis of Wavy Finned Absorber Solar Air Heater

Abhishek Priyam*[1], Prabha Chand* and Suresh Prasad Sharma*

Abstract **–** This paper deals with the analytical investigation on the energy and exergy analysis of wavy fin solar air heater. A mathematical model has been developed to evaluate the effect of various complex geometries of wavy fin such as fin spacing ratio, fin cross section aspect ratio and flow length ratio. The theoretical investigation showed that the exergy efficiency decreases with the increase in mass flow rate, increases, with the decrease in fin spacing ratio, flow cross section aspect ratio and flow length ratio. For the entire range of fin spacing ratio and cross sectional aspect ratio an optimum value of exergy efficiency has been found as 2.3% for the mass flow rate of 0.034kg/s-m^2 and corresponding rise in air temperature of 0.028K-m^2/W. Also, the results obtained from theoretical analysis of wavy finned solar air heater have been compared with the available experimental results of rectangular finned, triangular finned as well as a plane solar air heater.

Keywords – exergy analysis, exergy destruction, exergy efficiency, solar air heater, wavy fin.

1. INTRODUCTION

Energy is the most important resource to propel a country on the path of economic and industrial development. The energy demand is increasing with the increase in the human population and improvement in the living standard. The limited availability of fossil fuels and the environmental concern accumulated the researchers to focus their study on the renewable energies in the recent years. Solar energy is one of the optimistic renewable energy as it is clean, green, free best of all and the inexhaustible form of energy available on earth. Solar air heaters utilize solar radiation for a variety of purposes such as drying of agricultural products, space heating and air conditioning and industrial process heating. Apart from many advantages such as simple in design and maintenance, less leakage and corrosion, the low heat transfer coefficient between the absorber plate and air leads to its primary disadvantage and thus the low energy efficiency. An effective way to enhance heat transfer is the addition of fins in the direction of fluid flow. Various fin geometries, such as plane, wavy, offset strip, perforated and multi-louvered fins, they, apart from increasing the surface area density of solar air heater, also improve the convection heat transfer coefficients. Among these, wavy fins are considered as the most promising for their simplicity of manufacture and potential for better thermo hydraulic performance. A recent paper by Priyam and Chand [1] on the wavy finned solar air heater shows the effect of fin spacing and mass flow rate on the performances of wavy fin solar air heater. But the performance of wavy fin solar air heater depends on the complex geometry of wavy fin, such as corrugation aspect ratio (2A/L), fin spacing ratio (F_P/2A), flow length ratio (L_d/L) and flow cross-section aspect ratio (F_P/F_h). Also, various researchers [2]-[5] have studied the various configurations and designs of solar air heater to improve the energy efficiency. Based on the 1st law of thermodynamics, energy analysis may not be an intensive method due to the environmental conditions, losses and the irreversibility of the solar air heater. So, an analysis purely based on the second law of thermodynamics known as exergy analysis is required to determine the exergy of the system in addition to the energy analysis. Farzad and Emad [6] evaluated the energy and exergy performance of flat plate solar collector for a wide range of parameters. Results showed that the proper design with lower flow rate enhanced the overall performance. Yadav *et al.* [7] evaluated the exergy performance of solar air heater having an arc shaped oriented protrusions as roughness element. They also plotted the design plots to facilitate the designer to design such collector. Exergy evaluation of a single pass baffled solar air heater has been done by Sabzpooshani *et al.* [8]. They showed that exergy efficiency reduces sharply as the mass flow rate increases and increases with the increase in solar radiation. Bahrenmand *et al.* [9] developed a mathematical model to investigate on the energy and exergy analysis of different solar air collector systems with forced convection for a range of design parameters. They found that the system with fin and thin metal sheet were more efficient than other studied systems in terms of energy and exergy efficiency. They also found the negative values of exergy at very high Reynolds numbers for the systems with thin metal sheet and double glass covers. Gupta and Kaushik [10] studied various types of artificial roughness geometries on the absorber plate of solar air heater based on energy, exergy and effective efficiencies. They found that at high Reynolds number circular, vertical ribs and v-shaped ribs gave appreciable exergy efficiency while at low Reynolds number chamfered rib groove gave more exergy efficiency. Altfeld *et al.* [11] modeled the different types of solar air heater to study the energy performance and pressure drop in order to calculate net exergy flow. They optimized the design of absorbers and flow ducts by maximizing the net exergy flow and minimizing the

*Department of Mechanical Engineering, N.I.T Jamshedpur, Jharkhand-831014, India.

[1] Corresponding author;
Tel: + 91-8797181859
E-mail: priyamanik06@gmail.com.

exergy losses. The performance and entropy generation of double pass solar air heater having longitudinal fins were studied by Paisarn Naphon [12]. An experimental work to generate heat transfer and friction factor data for the flow in packed bed solar air heater was done by Laljee *et al.* [13]. Hikmet Esen [14] studied experimentally for the energy and exergy analysis of a double flow solar air heater having different obstacles on absorber plates. Results showed that the largest irreversibility was occurred in flat plate collector with lower efficiency. Energy and exergy analysis of solar air collector having various augmentation techniques has been done by Ucar and Inalli [15]. Largest irreversibility was reported with conventional solar collector with smallest collector efficiency. Kurtbas and Durmus [16] analyzed the efficiency and exergy of a new solar air heater. They found that heat transfer and pressure loss increased with the shapes and number of absorbers. Benli [17] studied five different types of solar air collectors experimentally to analyze the exergy and energy efficiency. Their data showed an enhancement in heat transfer and pressure drop with the shape of the absorber plate. Park *et al.* [18] analyzed the energy and exergy efficiency of typical energy systems. They found that exergy performance is lesser than the thermal performance. A review of exergy analysis of solar energy systems has been done by Kalogirou *et al.* [19]. Their analysis was useful in identification of irreversibilities in solar collectors alone as well as a complete cycle. The Exergy optimization method has been used by Nwosu [20] to design an absorber in a solar air heater.

The current study is focused with the theoretical analysis for the energy and exergy analysis of a sinusoidal wavy finned absorber solar air heater as well as a plane solar air heater. For a range of complex geometrical parameters such as fin spacing ratio, cross sectional aspect ratio, flow length ratio and the operating parameters such as mass flow rate and insolation, the effect of energy efficiency, air temperature rise, exergy destruction and exergy efficiency were determined and comparisons were made with plane solar air heater. In this way, by using wavy fin, the heat transfer increases along the flow line of air and changing the air velocity and pressure in the narrow extended area in which swirl and secondary flow forms and increases convective heat transfer coefficient.

2. THEORETICAL ANALYSIS

The considered solar heater consists of an absorber plate with attached wavy fins below the absorber. The schematic diagram of an examined solar air heater is shown in Figure 1 and its geometrical structure is shown in Figure 2. Bottom side of the solar air heater is perfectly insulated and the air is passed through the wavy finned absorber plate and bottom plate.

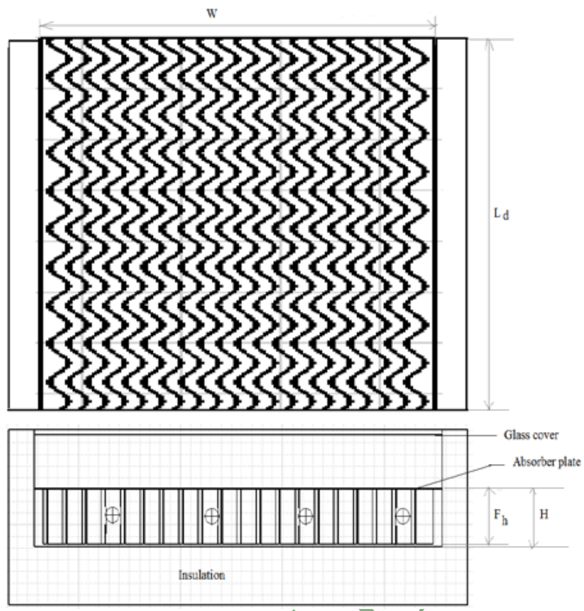

Fig. 1. Schematic diagram of wavy finned solar air heater.

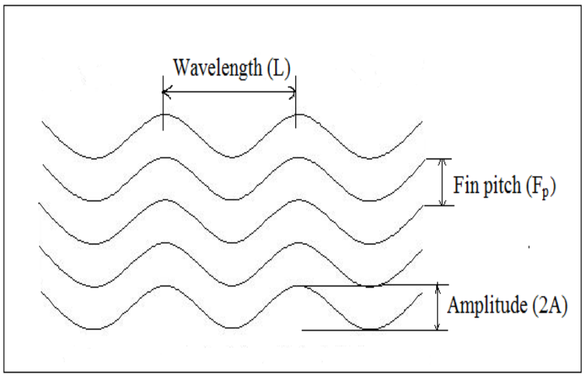

Fig. 2. Geometrical structure of wavy fin.

2.1 Energy Analysis

A very convenient expression for calculating the useful energy gain from a collector in terms of inlet fluid temperature, also known as Hottel-Whillier-Bliss equation [21] in terms of F_R, which represents the ratio of the actual useful heat gain rate to gain which would occur if the collector absorber plate is at inlet temperature.

$$Q_u = F_R A_p [I(\tau\alpha) - U_L (T_i - T_a)] \tag{1}$$

The useful heat gain rate for the collector can be expressed by considering increase in enthalpy of air flowing through the duct of the solar air heater as,

$$Q_u = \dot{m} C_p (T_o - T_i) \tag{2}$$

$$\text{also, } F_R = \frac{\dot{m} C_p (T_o - T_i)}{A_P [S - U_L (T_i - T_a)]} \tag{3}$$

Heat removal factor F_R can also be evaluated by using the following expression.

$$F_R = \frac{\dot{m} C_p}{U_L A_P}\left[1 - \exp\left(\frac{U_L A_P F'}{\dot{m} C_p}\right)\right] \tag{4}$$

where $$F' = \left(\frac{1+U_L}{h_e}\right)^{-1} \tag{5}$$

The total loss coefficient is the sum of top loss, bottom loss and side loss coefficients [22]:

and, $$U_L = U_t + U_b + U_s \tag{6}$$

An empirical relation for calculating the top loss coefficient is given by Klein [23];

where,

$$U_t = \left[\frac{N_{gc}}{\left(\frac{C}{T_{pm}}\right)\left(\frac{T_{pm}-T_a}{N_{gc}+f'}\right)^{0.33}} + \frac{1}{h_w}\right]^{-1} + \left[\frac{\sigma(T_{pm}^2+T_a^2)(T_{pm}+T_a)}{\frac{1}{\varepsilon_p+0.05N_{gc}(1-\varepsilon_p)} + \frac{2N_{gc}+f'+1}{\varepsilon_c} - N_{gc}}\right] \tag{7}$$

and

$$f' = (1+0.04h_w+0.0005h_w^2)(1+0.091N_{gc})$$

$$C = 365.9(1-0.00883\theta+0.0001298\theta^2)$$

$$h_w = 5.7+3.8V_w$$

$$U_b = \frac{K_{ins}}{\delta_{ins}} \tag{8}$$

$$U_s = \frac{(L+W)Hk_{ins}}{LW\delta_{ins}} \tag{9}$$

For a wavy finned solar air heater, the equivalent heat transfer coefficient is computed from Equation 10 and developed by Priyam *et al.* [1].

$$h_e = h_{fp} + \frac{2h_f\phi_f\beta_f h_{ff}}{w} + \frac{h_r h_{fb}}{h_r+h_{fb}} \tag{10}$$

For calculating the Nusselt number, the correlation for the Colburn factor(j) is recommended by Dong *et al.* [24] and used for wavy fin.

$$j = 0.0836\,\mathrm{Re}^{-0.2309}\left(\frac{F_p}{F_h}\right)^{0.1284}\left(\frac{F_p}{2.A}\right)^{-0.153}\left(\frac{L_d}{L}\right)^{-0.326} \tag{11}$$

where $j = Nu/Re.Pr^{1/3}$

Also, the correlation for f-factor given by Dong *et al.* [24]

$$f = 1.16\,\mathrm{Re}^{-0.309}\left(\frac{F_p}{F_h}\right)^{0.3703}\left(\frac{F_p}{2A}\right)^{-0.25}\left(\frac{L_d}{L}\right)^{-0.1152} \tag{12}$$

The pressure drop along the collector can be calculated for solar air heaters [23]

$$\Delta P = \frac{4fL_d\rho v^2}{2D_h} \tag{13}$$

The energy efficiency can be expressed in terms of

$$\eta_{en} = F_R\left[(\tau\alpha) - U_L\left(\frac{T_{fi}-T_a}{I}\right)\right] \tag{14}$$

3.2 Exergy Analysis

An overall exergy balance for the wavy finned solar air heater by considering a control volume as shown in Figure 3 (a) can be written as follows:

Exergy input of flowing air + Exergy of solar radiation falling on glass cover + Exergy of input work required by blower – Exergy output of flowing air
= irreversibility of air heating process.

or $$Ex_{in} + Ex_s + Ex_w - Ex_o = IR \tag{15}$$

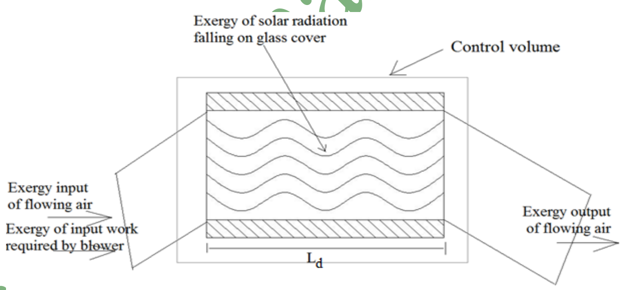

Fig. 3 (a). Exergy flow diagram of wavy finned solar air heater.

The irreversibility of the air heating process means exergy loss occurs because of the temperature difference among sun temperature and absorber plate and the heat losses due to ambient and pressure drop across the duct. The exergy input of flowing air can be given by

$$Ex_{in} = (h_i - h_a) - T_a(S_i - S_a) \tag{16}$$

and the exergy output of flowing air is given as

$$Ex_{out} = (h_0 - h_a) - T_a(S_0 - S_a) \tag{17}$$

Exergy of solar radiation falling on glass cover is given by [10]

$$Ex_S = IA_P\psi = IA_P\left(1-\frac{4}{3}\left(\frac{T_a}{T_s}\right)+\frac{1}{3}\left(\frac{T_a}{T_s}\right)^4\right) \tag{18}$$

where ψ represents the exergy efficiency of radiation.
Now, useful exergy gain by ignoring the pump work or the pressure drop.

$Ex_u = Ex_0 - Ex_{in}$

$$= (h_i - h_a) - T_a(S_i - S_a) - (h_0 - h_a) + T_a(S_0 - S_a) \tag{19}$$

Also, useful exergy gain when the pressure drop or pump work has been taken into consideration with an assumption that air is incompressible fluid or perfect gas, can be given as;

$$Ex_{up} = Ex_o - Ex_{in} - Ex_w$$

$$= \dot{m}C_p\left[\left(T_0 - T_i\right) - T_a \ln\left(\frac{T_0}{T_i}\right)\right] - \frac{T_a}{T_i}W_p \qquad (20)$$

The term Ex_w represents the exergy destruction due to pressure drop and given as;

$$Ex_w = \frac{T_a}{T_{in}}W_p \qquad (21)$$

The required pump work is given as;

$$W_p = \frac{\dot{m}\Delta p}{\rho\eta_{pm}} \qquad (22)$$

where η_{pm} is the pump motor efficiency and taken as 0.85.

The exergy efficiency, also called the second law efficiency (η_{II}) of the solar air heater can be calculated from [10].

$$\eta_{II} = \frac{Ex_{up}}{Ex_s} = \frac{mC_p\left[\left(T_0 - T_i\right) - T_a \ln\left(\frac{T_0}{T_i}\right)\right] - \frac{T_a}{T_i}W_p}{IAp\left(1 - \frac{4}{3}\left(\frac{T_a}{T_s}\right) + \frac{1}{3}\left(\frac{T_a}{T_s}\right)^4\right)} \qquad (23)$$

3.3. Steps for Calculation of Energy and Exergy Efficiency

For the study of energy and exergy efficiency of a wavy finned solar air heater, a C^{++} code has been developed by considering the following values of systems and operating parameters as shown in Table 1.

For the determination of energy and exergy efficiency the following procedure has been followed:

1. Initially an assumption of mean plate temperature has been done.
2. The values of U_L, F' , F_R, Q_u have been obtained with the assumed plate temperature and finally a modified value of mean plate temperature has been verified through the iterative process.
3. With the new values the various energy analysis parameters have been calculated.
4. The corresponding value of air outlet temperature has been calculated from Equation 3.
5. With the completion of step 4, the value of air outlet temperature has been used to calculate exergy efficiency from the Equation 20.

A flowchart representing the above procedure is shown in Figure 3 (b).

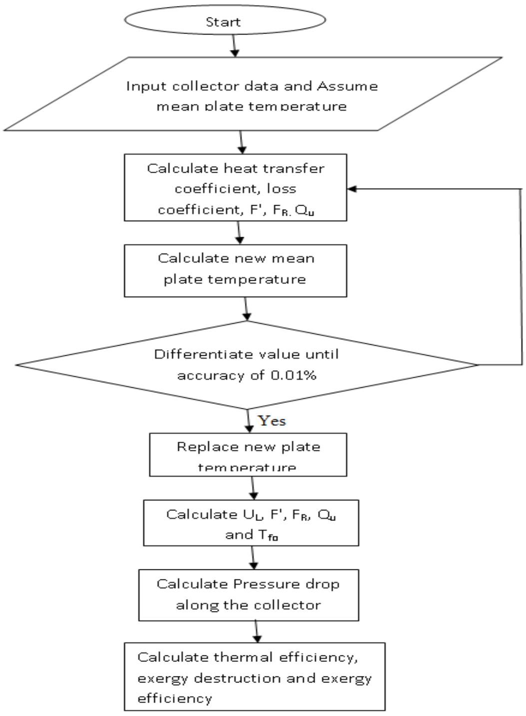

Fig. 3 (b). Flow chart for calculation of energy and exergy efficiency

Table. 1. Values of system and operating parameters.

Parameters	Value	Parameters	Value
W	1 m	T_s	5762 K
I	900 W/m^2	δ_{ins}	5 cm
H	2.5 cm	T_{fi}	30°C
δ_f	1 mm	ε_p	0.95
k_{ins}	0.1 W/m-K	ε_b	0.95
$(\tau\alpha)_e$	0.85	ε_c	0.88
k_a	0.029 W/m-K	V_w	2.5 m/s
$F_p/2A$	0.25 - 1	L_d/L	10 - 120
F_p/F_h	0.4 - 0.556	m	0.01-0.09 kg/s-m^2

4. VALIDATION OF THEORETICAL ANALYSIS

For the validation of the accuracy and reliability of the present results, comparisons of exergy efficiency among the results of the present study and those available in the literature have been made in Figure 4. The present results are compared with those of Bahrehmand *et al.* [9]. An enhancement of 1.84 times in exergy efficiency has been achieved with the use of wavy fins as compared to rectangular finned and triangular finned solar air heater, whereas 2.1 times enhancement has been observed with the plain solar air heater. Also, the average deviation of theoretical values of exergy efficiency is ±1. 57% of the experimental values of Bahrehmand *et al.* [9] and ±2.41% of the experimental values of Gupta and Kaushik [10]. This shows a good agreement between the present results and those available in the literature.

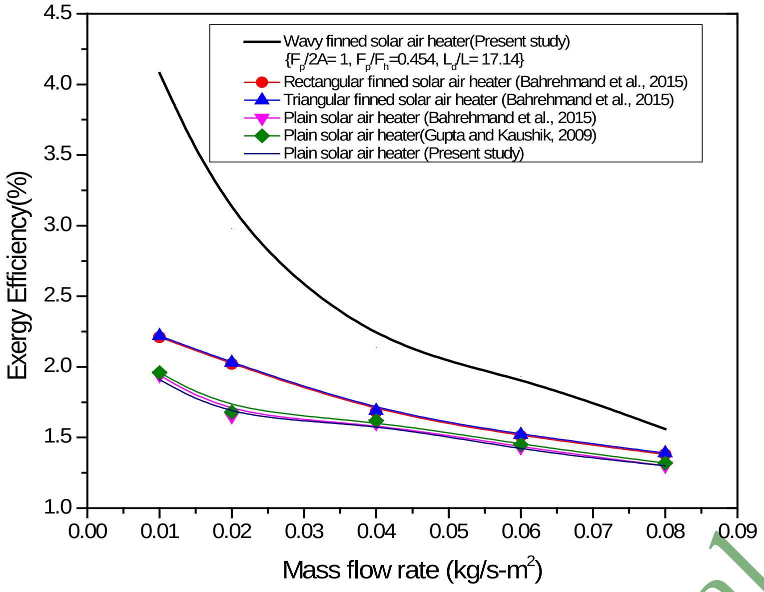

Fig. 4. Comparison of present work results with those available in the literature.

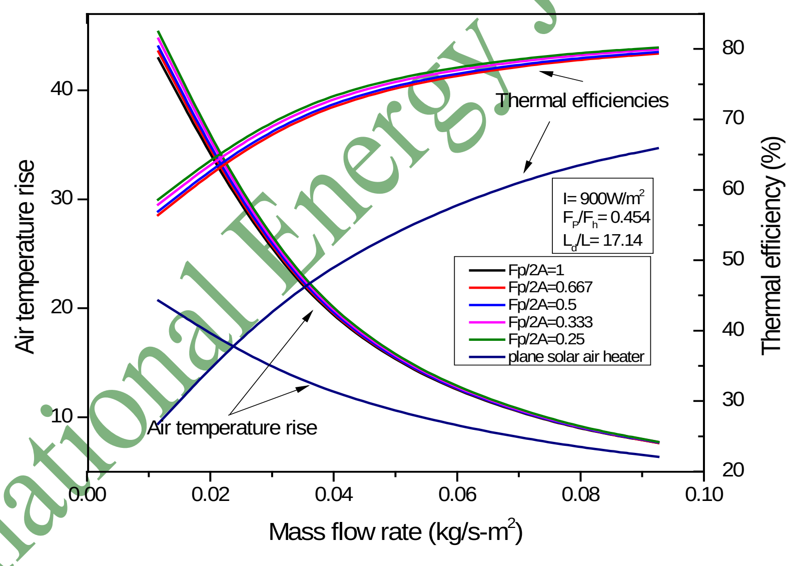

Fig. 5. Air temperature rise and energy efficiency as a function of mass flow rate for different fin spacing ratio.

5. RESULTS AND DISCUSSION

In the following section, the effects of the complex parameters such as fin spacing ratio, flow cross section aspect ratio, flow length ratio on the energy, exergy destruction and exergy efficiency are investigated on the mass flow rate and temperature rise parameter.

Figure 5 shows the air temperature rise and energy efficiency as a function of mass flow rate for different fin spacing ratio. For a specific mass flow rate air temperature and energy efficiency increases as the fin spacing ratio increases. Also, for a specific fin spacing ratio, air temperature decreases with increase in mass flow rate, whereas, energy efficiency increases. This is because of the large heat transfer rate in addition to larger surface area to the flowing air.

Figure 6 shows the variation of exergy destruction for the various fin spacing ratio and mass flow rate. The maximum exergy destruction of 38.5 W has been achieved at the maximum mass flow rate of 0.0925 kg/s and the minimum for spacing ratio of 0.25. For the entire fin spacing ratio, the exergy destruction increases with the increase in mass flow rate. This may be due to increase in mass flow rate leads to higher pressure drop. Figure 7 shows the exergy efficiency as a function of mass flow rate for different fin spacing ratio. It can be seen that the highest exergy efficiency is obtained at $F_P/2A = 0.25$ for mass flow rate less than 0.034 kg/s-m^2. Beyond this the reverse trend starts. This is because the increase in fin spacing ratio decreases the pressure drop. It can also be noted that for the entire range of $F_P/2A$, an optimum mass flow has been obtained at 0.034 kg/s-m^2 for the exergy efficiency of 2.3%.

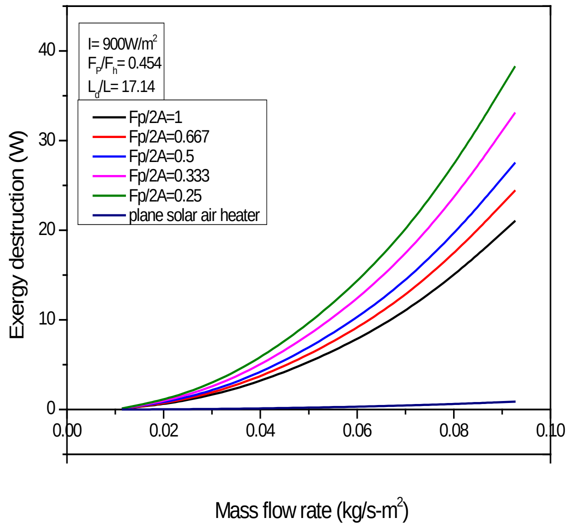

Fig. 6. Exergy destruction as a function of mass flow rate for different fin spacing ratio.

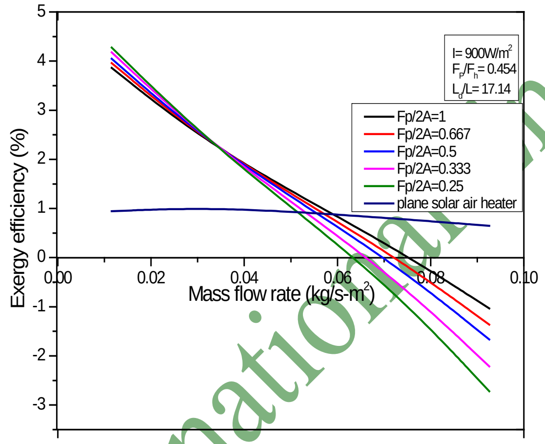

Fig. 7. Exergy efficiency as a function of mass flow rate for different fin spacing ratio.

Figure 8 shows that for all values of fin spacing ratio, $F_P/2A = 1$ shows the better exergy efficiency up to $\Delta T/I = 0.03\ K-m^2W$, beyond that reverse trend starts.

The maximum air temperature rise and exergy efficiency has been obtained for the lower fin spacing ratio of 0.25. This is because of the lower fin spacing ratio leads to narrower channel widths and the higher temperature rise leads to minimum flow velocities. For the entire range of $F_P/2A$, the optimum temperature rise has been found as 0.03 K-m^2/W with the corresponding exergy efficiency of 2.5%.

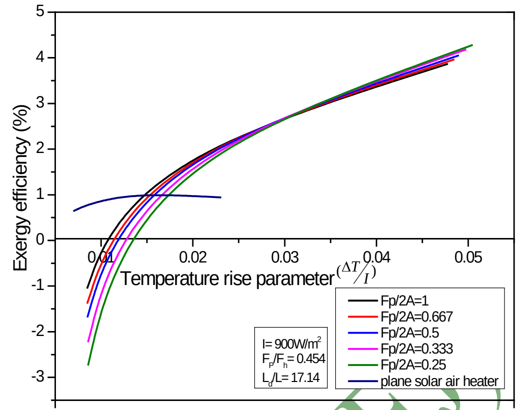

Fig. 8. Exergy efficiency as a function of temperature rise parameter for different fin spacing ratio.

Figure 9 represents air temperature rise and energy efficiency as a function of mass flow rate and flow cross section aspect ratio. Energy efficiency and air temperature increase with the decrease in flow cross section aspect ratio. Also, for a specific value of flow cross section aspect ratio, energy efficiency increases and air temperature rise decrease with the increase in mass flow rate. It is seen that with the increase in the cross-section aspect ratio, heat transfer increases and consequently the temperature depression results reduced heat transfer losses from the absorber plate to ambient air and hence an increase in efficiency.

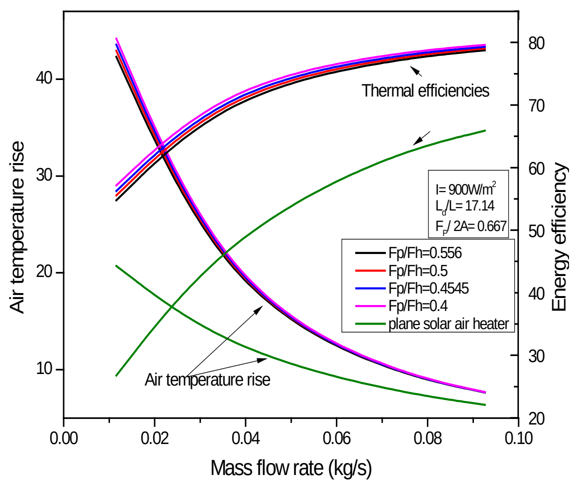

Fig. 9. Air temperature rise and energy efficiency as a function of mass flow rate and different aspect ratio.

Figure 10 shows the variation of exergy destruction for the various values of mass flow rate and various flow cross section aspect ratios. For a specific flow cross-section aspect ratio, increase in the mass flow rate decreases the energy destruction. Also the decrease in the flow cross-section aspect ratio increases the exergy destruction. The maximum exergy destruction of 41.9 W has been obtained for the lower mass flow rate of 0.0115 kg/s-m^2 and the flow cross section aspect ratio of 0.4. This is because of the increase in mass flow rate for a fixed flow cross section aspect ratio leads to decrease the pressure drop and the decrease in flow cross section aspect ratio leads to increased pressure drop.

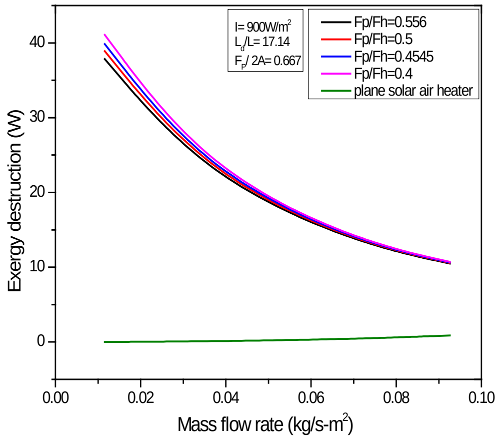

Fig. 10. Exergy destruction as a function of mass flow rate for different flow cross section aspect ratio.

Exergy efficiency as a function of mass flow rate and flow cross section aspect ratio has been plotted in Figure 11. It can be seen from the plot that the increase in flow cross section aspect ratio leads to decrease in exegetic efficiency up to the mass flow rate of 0.039 kg/s-m^2. Beyond that, increase in flow cross section aspect ratio results in increase in exergy efficiency. A maximum exergy efficiency of 4.2% has been achieved with the minimum flow cross section aspect ratio. This may because of minimum flow separation and formation of goethler vertices. For the investigated range of flow cross section aspect ratio, the optimum exergy efficiency of 1.9% has been achieved at the optimum mass flow rate of 0.039 kg/s-m^2.

It can be seen from Figure 12, the variation of temperature rise parameter on the exergy efficiency for the various flow cross section aspect ratios. Exergy efficiency increases with the increase in the temperature rise parameter for the entire range of flow cross section aspect ratio. Plane solar air heater also shows the same trend. Higher value of flow cross section aspect ratio shows the better exergy efficiency up to the temperature rise parameter of 0.026 K-m^2/W and thereafter it shows reverse trend upon increasing temperature rise parameter. This may be because of decreasing Fp/Fh, heat transfer area as well as energy conductance increases. An optimum value of rise in temperature of 0.026 K-m^2/W and exegetic efficiency of 2.6% has been achieved for the entire range of flow cross section aspect ratio.

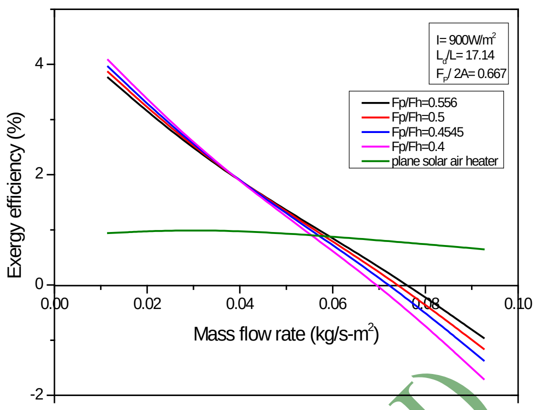

Fig. 11. Exergy efficiency as a function of mass flow rate for different flow cross section aspect ratio.

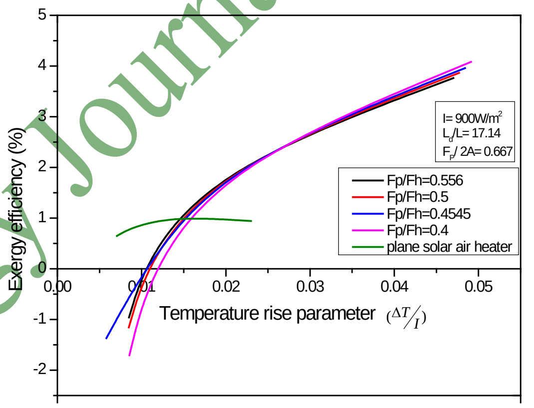

Fig. 12. Exergy efficiency as a function of temperature rise parameter for different flow cross section aspect ratio.

Figure 13 shows the air temperature rise and energy efficiency as a function of mass flow rate for different flow length ratio. Energy efficiency and temperature rise increases with the decrease in the flow length ratio. Also, for a specific value of the flow length ratio, temperature rise decreases and energy efficiency increases with the increase in mass flow rate. This may be because of the increase in flow length ratio leads lesser heat transfer rate and higher energy losses.

Figure 14 shows the exergy destruction as a function of mass flow rate and flow length ratio. It can be seen from a plot that decreasing the flow length ratio leads to increase in exergy destruction. This may be due to increase in the flow length ratio leads to higher pressure drop. Also, for a specific flow length ratio increasing the mass flow rate decreases the exergy destruction and leads to higher pressure drop. The plane solar air heater almost remains constant throughout the entire range of mass flow rate. Figure 15 shows the exergy efficiency for the entire range of mass flow rate for different flow length ratio. Exergy efficiency decreases with the increase in the flow length ratio, as the pressure drop increased with the decrease in the flow length ratio. For a specific flow length ratio, exergy efficiency decreases as the mass flow rate increases. The wavy fin solar air heater showed better exergy efficiency up to the mass flow rate of 0.061 kg/s-m^2.

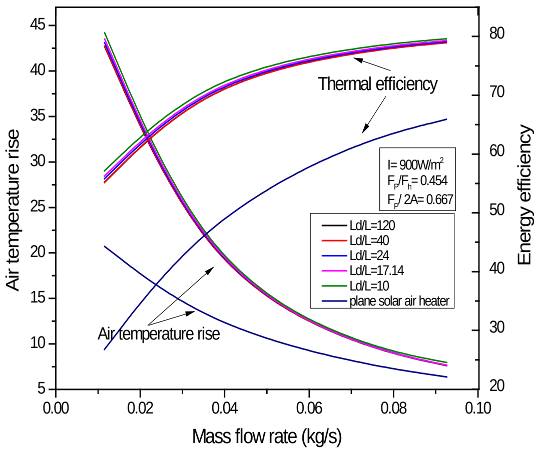

Fig. 13. Air temperature rise and energy efficiency as a function of mass flow rate for different flow length ratio.

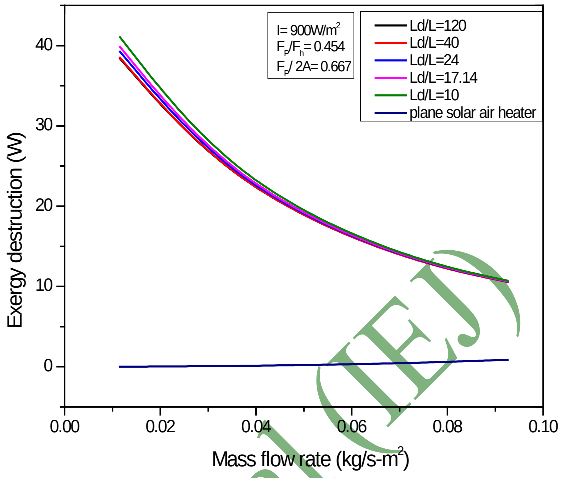

Fig. 14. Exergy destruction as a function of mass flow rate for different flow length ratio.

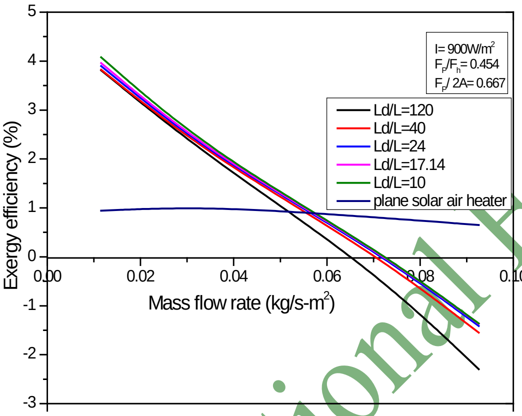

Fig. 15. Exergy efficiency as a function of mass flow rate for different flow length ratio.

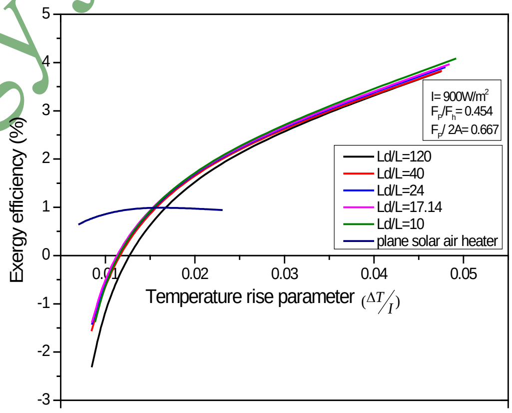

Fig. 16. Exergy efficiency as a function of temperature rise parameter for different flow length ratio.

Figure 16 shows the exergy efficiency as a function of temperature rise parameter for different flow length ratio. Exergy efficiency increases with the decrease in the flow length ratio. For a particular value of the flow length ratio, increasing the temperature rise parameter increases the exergy efficiency. Beyond the temperature rise parameter of 0.016 K-m^2/W that the wavy fin solar air heater shows the better exergy efficiency. This shows that up to 0.016 K-m^2/W, the effect of pressure drop is overcome by the heat transfer rate and beyond that the pressure drop increases.

Values of the exergy efficiency at all mass flow rates are low mainly because of high exergy loss from absorption of solar radiations by absorber plate. At higher mass flow rates the exergy efficiency becomes negative because at higher mass flow rates required pump work exceeds the exergy of heat energy collected and the net exergy flow becomes negative.

Figure 17 shows the values of fin spacing ratio as a function of the temperature rise parameter. For fin spacing ratio less than 0.33, the temperature rise parameter is independent of insolation. However, for the range of temperature rise parameter between 0.0475- 0.0497 m^2-K/W, the value of fin spacing ratio is a function of insolation.

Figure 18 shows the plot for flow cross section aspect ratio as a function of the temperature rise parameter. For the range of temperature rise parameter between 0.047-0.0496 m^2-K/W, flow cross section aspect ratio is a function of solar radiation. Also, increasing the flow cross section aspect ratio reduces the temperature rise parameter.

Figure 19 shows the value of the flow length ratio as a function of the temperature rise parameter. Beyond the temperature rise parameter of 0.0487 m^2-K/W, the value of the flow length ratio is independent of insolation. However, temperature rise parameter below 0.0487, the flow length ratio is a function of insolation.

Solar air heater having investigated type of complex wavy fin geometry can be designed based upon exergy efficiency. For a known collector size, initially the required temperature rise of flowing air through the duct of solar air heater is to be decided. After knowing the solar radiation of the place where the solar air heater has to be installed, the temperature rise can be calculated. By knowing the temperature rise parameter, insolation and the collector area corresponding $F_P/2A$, F_P/F_h and L_d/L of wavy fin can be calculated for maximum exergy efficiency from design plots.

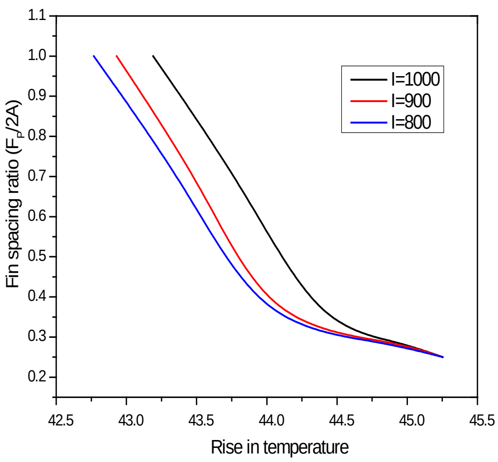

Fig. 17. Fin spacing ratio as a function of the air temperature rise for different insolation.

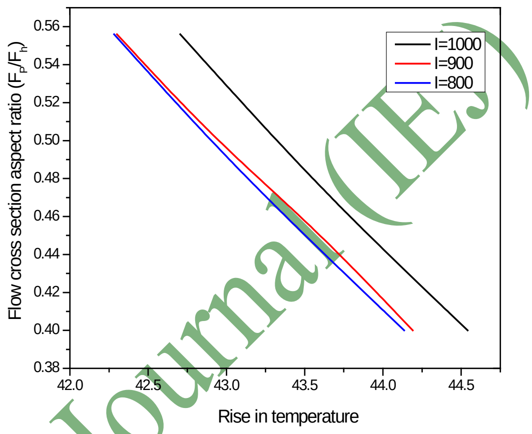

Fig. 18. Flow cross section aspect ratio as a function of air temperature rise for different insolation.

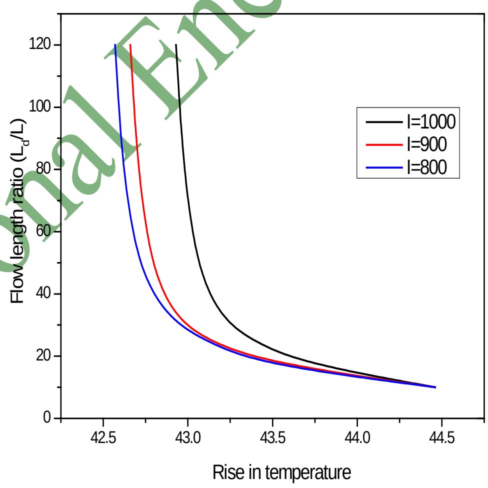

Fig. 19. Flow length ratio as a function of air temperature rise for different insolation.

6. CONCLUSIONS:

Attachment of wavy fins below the absorber plate is one of the effective techniques to enhance the heat transfer rate in solar air heater as the wavy fins increases the heat transfer area simultaneously increasing the heat transfer coefficient due to the shape of the wavy fin [1]. In this study, energy and exergy analysis on the complex geometries of the wavy fin such as fin spacing ratio, flow cross section aspect ratio, flow length ratio has been investigated theoretically. Based on the results and discussion following conclusions can be drawn:

1. Use of wavy fins below the absorber plate has been considered as an effective technique for performance enhancement based on exergy analysis.
2. For the higher fin spacing ratio of 1, the exergy destruction has been found to be maximum as 38.5 W at a higher mass flow rate of 0.0925 kg/s-m^2, whereas for the lower flow cross section aspect ratio of 0.4, exergy destruction has been

found to be maximum of 41 W and for lower flow length ratio of 10, exergy destruction has been found to be 41.09 W at the mass flow rate of 0.011 kg/s-m^2.

3. For the range of fin spacing ratio, mass flow rate lesser than 0.055 kg/s-m^2 shows the better exergy efficiency and the optimum value of exergy efficiency has been found as 2.3% for the mass flow rate of 0.034 kg/s-m^2 and corresponding temperature rise of 0.028 K-m^2/W for the entire range of fin spacing ratio.
4. For the range of flow cross section aspect ratio and mass flow rate lower than 0.062 kg/s-m^2, better exergy efficiency has been found and the optimum value of exergy efficiency of 2.3% at the mass flow rate of 0.034 kg/s-m^2 and corresponding temperature rise of 0.028 K-m^2/W for the entire range of flow cross section aspect ratio.
5. For the range of flow length ratios and mass flow rate lower than 0.063 kg/s-m^2, the exergy efficiency has been found better. Exergy efficiency increases with the decrease in the flow length ratio also the temperature rise parameter increases.
6. It has been found that the exergy efficiency of plane solar air heater is almost constant for the entire range of mass flow rate and more than those of wavy fin solar air heater at the high mass flow rates.
7. Lower values of fin spacing ratio, fin cross section aspect ratio and flow length ratio are recommended for higher temperature rise for the investigated range of system and operating parameters.

NOMENCLATURE

2A	Twice amplitude of wavy fin (mm)
A_p	Area of absorber plate (m^2)
C_p	Specific heat at constant pressure (J/kgK)
F_h	Height of fin (m)
$F_p/2A$	Fin spacing ratio
F_p/F_h	Flow cross section aspect ratio
H	Spacing between absorber plate and bottom plate (m)
h	Specific enthalpy
h_e	Effective heat transfer coefficient (W/m^{2}K)
H_w	Wind heat transfer coefficient (W/m^{2}K)
I	Intensity of Solar radiation (W/m^2)
k_a	Energy conductivity of air (W/mK)
k_{ins}	Energy conductivity of insulating material (W/mK)
L_d	Length of the collector/ Absorber plate (m)
L_d/L	Flow length ratio
N_{gc}	Number of glass covers
Q_u	Useful energy energy gain (W/m^2)
S	Specific entropy
T_a	Ambient Temperature (°C)
T_{fi}	Inlet air temperature (°C)
T_o	Outlet air temperature (°C)
Ts	Sun Temperature(K)
U_b	Bottom loss coefficient (W/m^{2}K)
U_L	Total loss coefficient (W/m^{2}K)
F'	Collector efficiency factor
Re	Reynolds number
Pr	Prandtl number
U_t	Top loss coefficient (W/m^{2}K)
V_w	Wind velocity (m/s)
W	Width of the collector/ Absorber plate (m)
F_R	Collector heat removal factor
$\dot{m}$	Mass flow rate (kg/hr)
δ_f	Thickness of fin (m)
ΔP	Pressure drop (N/m^2)
δ_{ins}	Thickness of insulation (m)
ρ	Density of air (kg/m^3)
L	Wavelength of wavy fin (mm)
η_{II}	Exergy efficiency
β	Area enhancement factor
η_{en}	Energy efficiency
F_P	Fin pitch (mm)

REFERENCES

[1] Priyam A. and P. Chand. 2016. Energy and thermohydraulic performanceof wavy finned absorber solar air heater. *Solar Energy* 130: 250-259.

[2] Karim M.A. and M.N.A. Hawlader. 2006. Performance investigation of flat plate, v-corrugated and finned air collectors. *Energy* 31: 452-470.

[3] Hans V.S., Saini R.P., Saini J.S. 2010. Heat transfer and friction factor correlations for a solar air heater duct roughened artificially with multiple v-ribs. *Solar Energy* 84(6): 898-911.

[4] Choudhary C. and H.P. Garg. 1991. Design analysis of corrugated and flat plate solar air heaters. *Renewable Energy* 1(5/6): 595-607.

[5] El-Sebaii A.A, Aboul-Enein S., Ramadan M.R.I., Shalaby S.M., and Moharram B.M., 2011. Energy performance investigation of double pass finned plate solar air heater. *Applied Energy* 88(5): 1727-1739.

[6] Jafarkazemi F. and E. Ahmadifard. 2013 Energy and exergy evaluation of flat plate solar collectors. *Renewable Energy* 56: 55-63.

[7] Yadav S., Kaushal M., Varun, and Siddhartha. 2014. Exergy performance evaluation of solar air heater having arc shape oriented protrusions as roughness element. *Solar Energy* 105: 181-189.

[8] Sabzpooshani M., Mohammadi K., and Khorasanizadeh. 2014. Exergy performance evaluation of a single pass baffled solar air heater. *Energy* 64: 697-706.

[9] Bahrehmand D., Ameri M., and Gholampour M. 2015. Energy and exergy analysis of different solar air collector systems with forced convection. *Renewable Energy* 83: 1119-1130.

[10] Gupta M.K. and S.C. Kaushik. 2009. Performance evaluation of solar air heater for various artificial roughness geometries based on energy, effective and exergy efficiencies. *Renewable Energy* 34: 465-476.

[11] Altfeld K., Leiner W., and Fiebig M., 1988. Second law optimization of flat plate solar air heaters. *Solar Energy* 41(2): 127-132.

[12] Naphon P., 2005. On the performance and entropy generation of the double-pass solar air heater with longitudinal fins. *Renewable Energy* 30: 1345-1357.
[13] Lalji M.K., Sarviya R.M., and Bhagoria J.L., 2012 Exergy evaluation of packed bed solar air heater. *Renewable and Sustainable Energy Reviews* 16: 6262-6267.
[14] Esen H., 2008 Experimental energy and exergy analysis of a double flow solar air heater having different obstacles on absorber plates. *Building and Environment* 43: 1046-1054.
[15] Ucar A. and M. Inalli. 2006 Energy and exergy analysis of solar air collectors with passive augumentation techniques. *Int. Communications in Heat and Mass Transfer* 33: 1281-1290.
[16] Kurtbas I. and A. Durmus. 2004. Efficiency and exergy analysis of a new solar air heater. *Renewable Energy* 29: 1489-1501.
[17] Benli H., 2013. Experimentally derived efficiency and exergy analysis of a new solar air heater having different surface shapes. *Renewable Energy* 50: 58-67.
[18] Park S.R., Pandey A.K., Tyagi V.V., and Tyagi S.K., 2014 Energy and exergy analysis of typical renewable energy systems. *Renewable and Sustainable Energy Reviews* 30: 105-123.
[19] Kaloogirou S.A., Karellas S., Badescu V., and Braimakis K., 2016. Exergy analysis on solar energy systems: A better understanding of their sustainability. *Renewable Energy* 85: 1328-1333.
[20] Nwosu P.N., 2010 Employing exergy-optimized pin fins in the design of an absorber in a solar air heater. *Energy* 35: 571-575.
[21] Duffie J.A. and W.A. Beckman. 2006. *Solar Engineering of Energy Processes*, 3rd Edition. Wiley Interscience, New York.
[22] Krieder J.F. and Krieth. 1978. *Principles of Solar Engineering*, 2nd Edition. McGraw Hill Book Company, New York.
[23] Mc Adams, 1954. W.H. Heat Transmission. McGraw -Hill Company, New York.
[24] Junqi D., Chen J., Chen Z., Zhou Y., Wenfeng Z., 2007. Heat transfer and pressure drop correlations for the wavy fin and flat tube heat exchangers. *Applied Thermal Engineering* 27 (11–12): 2066–2073.